Journal of Chromatography A, 1218 (2011) 2189–2195

Contents lists available at ScienceDirect

Journal of Chromatography A

journal homepage: www.elsevier.com/locate/chroma

Preparation of molecularly imprinted polymers for the selective recognition of the bioactive polyphenol, (*E*)-resveratrol

Lachlan J. Schwarz, Basil Danylec, Simon J. Harris, Reinhard I. Boysen, Milton T.W. Hearn*

Centre for Green Chemistry, Monash University, Clayton, 3800 Vic, Australia

ARTICLE INFO

Article history:
Received 3 November 2010
Received in revised form 16 February 2011
Accepted 16 February 2011
Available online 23 February 2011

Keywords:
Resveratrol
Polyphenols
Solid phase extraction
Molecular modelling
Molecularly imprinted polymers

ABSTRACT

(*E*)-Resveratrol imprinted polymers have been rationally designed with the aid of molecular modelling and NMR spectroscopic titration techniques to determine the optimal ratio of the template to functional monomer for polymer formation. Based on this approach, (*E*)-resveratrol imprinted polymers were prepared *via* non-covalent self-assembly with the functional monomer 4-vinylpyridine (4VP) in a 1:3 molar ratio. Polymerisation in the presence of a cross-linker resulted in rigid block copolymers that had selective capacities towards (*E*)-resveratrol (e.g. 14 μmol/g) when compared to the non-imprinted reference polymer. The selectivity of these MIPs was also examined using several structurally related polyphenolic compounds to determine the influence of polyphenolic hydroxyl number and position on binding and molecular recognition.

1. Introduction

Phytochemicals present in foodstuffs are an important group of compounds that can contribute to mammalian health and wellbeing [1]. Within this genre, relatively simple polyphenols, exemplified by the hydroxylated stilbene (*E*)-resveratrol **1**, have attracted considerable interest because of their reported anti-aging [2–5], anticancer [6–9], anti-inflammatory [10,11] and cardioprotective effects [12–15]. (*E*)-Resveratrol is a natural product of low molecular mass arising as an early product from the biosynthesis of phenylalanine. It is also thought to be an intermediate leading to some of the structurally more complicated polyphenols and flavonoids [16]. Nature has adapted this molecule as a phytoalexin in plants to protect against fungal attack [17,18] and injury such as that caused by exposure to ultra-violet light [18].

Two of the primary dietary sources of (*E*)-resveratrol are from peanuts and grapes, and their processed derivatives such as peanut butter and wine. These sources contain variable concentrations of resveratrol as a consequence of numerous factors, including climate, exposure to infection and their cultivar strain [19,20]. For instance, (*E*)-resveratrol concentrations in red wine have been reported to range from 0.6 to 8.0 mg/L [21,22], in white wines 0.031–0.122 mg/L [21,22], and dry grape skins between 21.5 and 174.0 μg/g [23,24].

At these concentrations, the detection and quantitative determination of these naturally occurring molecules has generally been reliant on liquid/liquid separation methods followed by analytical techniques such as high-performance liquid chromatography (HPLC). However, in many cases, the analysis of very complex samples with one single mode of chromatography cannot provide sufficient resolution to enable the quantification of target analytes based on chromatographic peak areas. Therefore, there is a need to develop techniques for the rapid and selective analysis of such important bioactives. Two- or multi-dimensional liquid chromatography could provide such resolution, but at the expense of significant material losses and increased costs with each additional chromatographic step. Similar considerations of the analysis of specific target analytes from complex feedstocks govern their preparative extraction. For both the analysis and purification of natural products from complex feedstocks, an elegant solution would be a two-step protocol comprising high capacity affinity chromatography followed by a high resolution reversed-phase chromatographic separation. In this context, affinity chromatography materials based on molecularly imprinted polymers (MIPs) could be employed as a solid phase extraction step for both analytical and preparative purposes. A further advantage of these new materials is their potential for bioactive enrichment *via* scalable processes as industrial applications.

MIPs are functional porous materials possessing cavities with a pre-defined selectivity for a particular target molecule. They have found a broad range of applications including synthesis and catalysis [25], controlled drug delivery systems [26], sensors [27] and separations [25,28]. High affinity binding sites are generated by first

* Corresponding author. Tel.: +61 3 9905 4547; fax: +61 3 9905 8501.
E-mail address: milton.hearn@monash.edu (M.T.W. Hearn).

0021-9673/$ – see front matter © 2011 Elsevier B.V. All rights reserved.
doi:10.1016/j.chroma.2011.02.043

Table 1
Summary of the MIP synthetic preparations used in this investigation.

Polymer code	(*E*)-Resveratrol (template)	4VP (FM)	EGDMA (cross-linker)	Porogen
P1*	1 mmol	3 mmol	15 mmol	CH_3CN/EtOH 5:1 (v/v)
N1*	None	3 mmol	15 mmol	CH_3CN/EtOH 5:1 (v/v)
P2	1 mmol	None	15 mmol	CH_3CN/EtOH 5:1 (v/v)
N2	None	None	15 mmol	CH_3CN/EtOH 5:1 (v/v)

All polymerisations were initiated with AIBN and the reaction carried out at 50 °C for 24 h.
* Prepared with an additional 24 h thermal annealing at 60 °C.

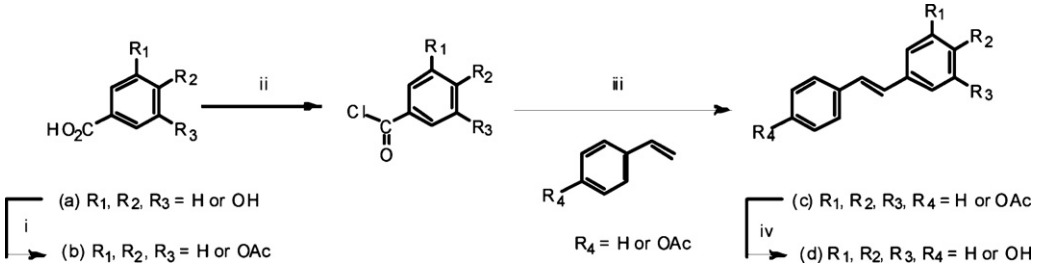

Fig. 1. Synthetic routes for the preparation of (*E*)-resveratrol and other polyphenols. Reagents and conditions: Yields shown in parentheses are typical for (*E*)-resveratrol. (i) Ac_2O, pyr, DMAP, EtOAc, 0–40 °C, 2 h, (72%), or Ac_2O, Et_3N, EtOAc, reflux, 4 h, (34%); (ii) $SOCl_2$, DMF, toluene, 100 °C, 3 h, (100%); (iii) 2% $Pd(OAc)_2$, NEM, toluene, reflux, overnight, (51%); (iv) (a) KOH, MeOH, reflux, 60 min, then (b) HCl(aq), (79%), or TsOH, MeOH, 85 °C, overnight, (95%).

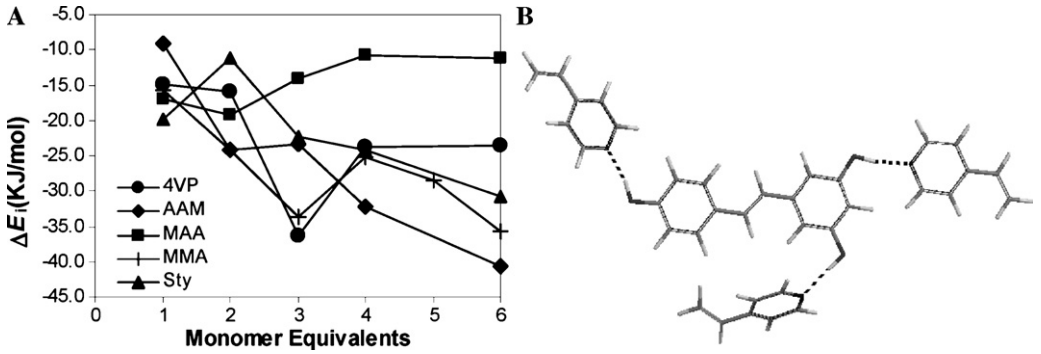

Fig. 2. (A) Modelling titration data for (*E*)-resveratrol against the functional monomers 4-vinylpyridine (4VP, ●), acrylamide (AAM, ♦), methacrylic acid (MAA, ■), methylmethacrylate (MMA, +) and styrene (Sty, ▲) showing predicted ΔE_i values for monomer equivalents ranging from 1 to 6. (B) Molecular modelling image of Spartan generated complex between (*E*)-resveratrol and 3 units of 4VP demonstrating O–H···N hydrogen bonding (dashed lines).

forming either a covalent or a non-covalent pre-association complex between a template molecule and an appropriate functional monomer. This complex is then trapped within a highly cross-linked polymeric matrix. Removal of the template molecule creates a polymer cavity with appropriately positioned functional groups capable of molecular recognition *via* complementary interactions with a target molecule.

In this paper, we report the design and preparation of a (*E*)-resveratrol imprinted polymer *via* the non-covalent self-assembly of specific functional monomer units and the assessment of

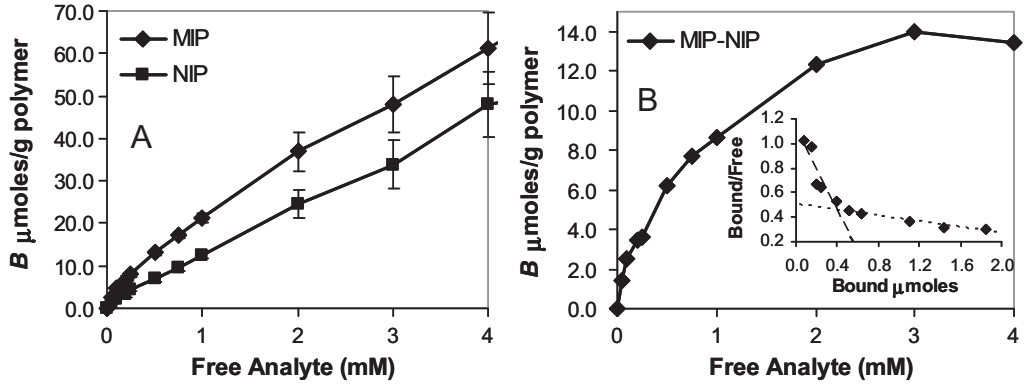

Fig. 3. (A) Static binding isotherms for the binding of (*E*)-resveratrol with multiple batches of P1. Measurements were determined in duplicate with a minimum of 3 replicates. Error bars indicate the standard error of the mean (SEM). (B) Selective capacity of the MIP for (*E*)-resveratrol: the inset shows the binding data in a Scatchard plot [36] format.

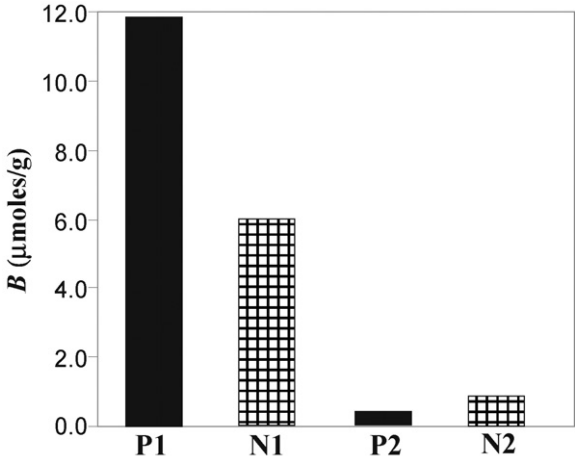

Fig. 4. Binding performance of imprinted and non-imprinted polymers towards (*E*)-resveratrol under static conditions.

its selectivity for (*E*)-resveratrol compared to structurally similar analogues, utilising *inter alia* molecular modelling and NMR spectroscopic titration techniques to determine optimal ratios of the template to functional monomer for polymer formation. (*E*)-Resveratrol was chosen as a relevant bioactive candidate to investigate this approach for the development of a generic strategy to prepare non-covalent molecularly imprinted polymer materials for the selective capture and separation of polyphenols. (*E*)-Resveratrol is a rigid small molecule that has three phenolic substituents capable of hydrogen bonding, and two aromatic regions capable of donor–acceptor, π–π stacking or hydrophobic interactions. These functionalities have been exploited for the creation of polyphenol selective binding cavities in MIP materials and to enable the influence of polyphenolic hydroxyl number and position on binding to be determined.

2. Materials and methods

2.1. Reagents

Resveratrol-3-*β*-D-glucopyranoside (3,4′,5-trihydroxystilbene-3-*β*-D-glucopyranoside) **5**, (*E*)-stilbene **8**, 4-vinylpyridine (4VP), acrylamide (AAM), methacrylic acid (MAA), methylmethacrylate (MMA), styrene, ethyleneglycol dimethacrylate (EGDMA) and 2,2′-azobis(2-methylpropionitrile) (AIBN) were purchased from Sigma–Aldrich (Sydney, Australia). All solvents used for MIP preparation and evaluation were HPLC grade. The preparation of (*E*)-resveratrol **1** and its analogues **2**–**7** was adapted from procedures previously described [29,30].

2.2. Equipment

An Agilent Technologies 1100 LC system (Waldbronn, Germany) consisting of a binary pump with a vacuum degasser, auto-sampler with a 900 μL sample loop, thermostated column compartment and a diode-array detector was employed for the HPLC separation of the sample. Injected samples were analysed by RP-HPLC on a Zorbax Eclipse XDB-C18 column (4.6 mm × 150 mm, 5 μm particle size).

2.3. Molecular modelling

All modelling calculations were conducted using Spartan'08 for Windows V100 software package on a Pentium IV 2.0 GHz. Modelling procedures were based on previously described methods [31], whereby the semi-empirical equilibrium geometry level theory was applied using a PM3 force field to calculate the energy of formation values (ΔH_f), for template, monomer clusters and monomer-template clusters in the gas phase without consideration of solvent effects. Monomer cluster sizes ranging from 1 to 6 monomer units were modelled and the ΔH_f values determined for the interaction of the monomer with itself at these cluster sizes. The (*E*)-resveratrol structural file was then inserted into each cluster file with no pre-defined orientation imposed upon either template or monomer cluster. Equilibrium geometry was determined using an iterative approach. A minimum of three iterations yielded theoretical estimates of the average energy of formation (ΔE_i) for the complex, which was determined using the following equation:

$$\Delta E_i = \Delta H_{f\_Complex}(\Delta H_{f\_Template} + \Delta H_{f\_Monomer})$$

2.4. ^{1}H NMR spectroscopy titrations

The following procedure is representative of the general approach that has been deployed for these ^{1}H NMR spectroscopy titration experiments. (*E*)-Resveratrol (23 mg, 0.1 mmol) dissolved in trideuteroacetonitrile (CD_3CN) was titrated with increasing molar equivalents of 4-vinylpyridine. The ^{1}H NMR spectrum was recorded after each addition and the change in aromatic –OH shifts followed until the presence of H bonding interactions was evidenced by the consistent downfield shift of this aromatic –OH signal with increased additions. This process was continued until the aromatic –OH signal was no longer detectable due to peak broadening.

2.5. MIP preparation

MIPs were prepared by dissolving the template, e.g. (*E*)-resveratrol (228 mg, 1 mmol) in acetonitrile/ethanol (6 mL, 5:1, v/v) in end-capped glass reaction tubes to which the functional monomer 4VP (322 μL, 3 mmol) was added. The mixture was sonicated for 10 min and the cross-linker EGDMA (2.314 mL, 15 mmol) and the free radical initiator AIBN (51 mg, 0.31 mmol) then added. This pre-polymerisation mixture was sparged with N_2 gas for 5 min and then placed in a thermostatic water bath at 50 °C for 24 h. A number of polymer samples were further annealed by heating at 60 °C for time intervals up to 24 h. The polymers were then removed from the reaction tubes, crushed and ground using a Retsch 200 ball mill. The ground particles were subsequently sieved. In all subsequent work, particles of 63–100 μm size were employed. Fines were removed by repeated cycles of suspension of the polymer particles in acetone and decanting the supernatant. The (*E*)-resveratrol template was removed from the MIP resin by at least three washings in methanol containing 10% acetic acid by volume (50 mL) with gentle stirring. The washings were monitored by UV–vis spectroscopy at 321 nm and continued until the UV absorption at 321 nm reached zero and (*E*)-resveratrol could no longer be detected. MIPs were then washed with methanol to remove traces of acetic acid, filtered and dried *in vacuo*. Non-imprinted control polymers (NIPs) were prepared in exactly the same manner but in the absence of the template molecule. A summary of various conditions employed for the preparation of the MIPs and NIPs is given in Table 1.

2.6. MIP evaluation

Batch binding studies with (*E*)-resveratrol in acetonitrile were conducted over the concentration range of 0–4 mM using both MIPs and NIPs and constant polymer weight. Polymer (30 mg) was weighed into sealable Eppendorf tubes (1.7 mL) and incubated at 20 °C with the analyte solution (1.5 mL, 0–4 mM) on a rotary mixer at 40 rpm for 18 h. The mixture was centrifuged at 13,000 rpm for

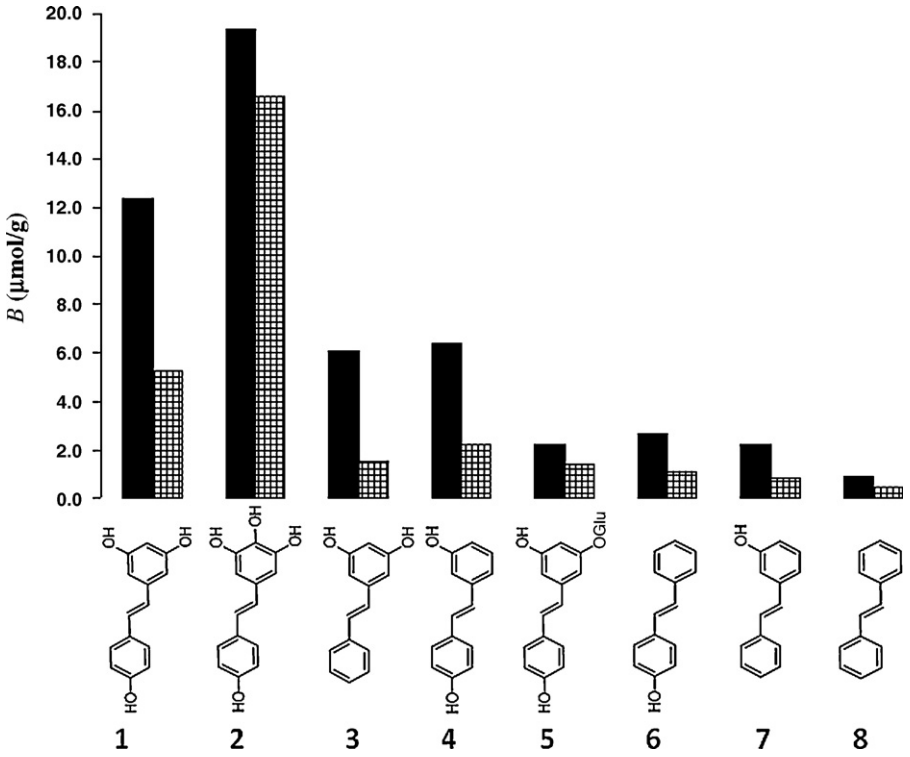

Fig. 5. Static binding B_{max} values from single analyte binding experiments showing the amount of bound analyte per gram of polymer for (*E*)-resveratrol, **1**, and seven polyhydroxy stilbene structural analogues, **2**–**8**, by the MIP P1 (black) and the NIP control N1 (hatched).

15 min to pellet the ligand-bound polymer complex. An aliquot (200 μL) of the supernatant was removed and analysed by RP-HPLC with UV detection at 321 nm. The concentration of unbound (*E*)-resveratrol was determined from a linear 5-point calibration curve. Subtraction of this value from the initial total analyte concentration gave the amount of analyte bound (*B*), expressed as μmol/g polymer. To investigate non-specific surface binding, static binding assays were further conducted on both the MIP and NIP in parallel. The polymer (30 mg) was weighed into sealable Eppendorf tubes (1.7 mL) and a (*E*)-resveratrol solution (1.5 mL, 0.5 mM in acetonitrile) added. The resulting mixture was then treated and analysed as described above.

3. Results and discussion

3.1. Selection of the analogues of (E)-resveratrol

The selected analogues were chosen on their basis to enable the comparative examination of the number of potential binding sites and their relative structural orientations, based around the central *E*-stilbene core of (*E*)-resveratrol. The general synthetic procedure to prepare these compounds is summarized in Fig. 1. A detailed description of the preparation of (*E*)-resveratrol, **1**, adapted from the early methodology [30], and the hydroxylated stilbene analogues (*E*)-5-(4-hydroxy-styryl)benzene-1,2,3-triol **2**, (*E*)-5-styrylbenzene-1,3-diol **3**, (*E*)-3-(4-hydroxy-styryl)phenol **4**, (*E*)-4-styrylphenol **6**, (*E*)-3-styrylphenol **7** (and other polyphenols) has been reported [29] elsewhere. The process entailed conversion of a functionalized benzoic acid to its more activated acid chloride, which after removal of the solvents by distillation, was immediately reacted with an appropriate styrene. The coupling reaction, promoted with catalytic amounts of palladium acetate, reportedly [30] proceeds *via* a chalcone intermediate. However, under the conditions employed in our investigations only the stilbene adduct was isolated, indicating that complete decarbonylation occurs simultaneously during the reaction. The *E* stereochemistry of the product was readily confirmed by the characteristic J_{trans} = 16 Hz coupling constant in the ^{1}H NMR and no *Z* isomer was detected (expected J_{cis} = ≤12 Hz).

3.2. Molecularly imprinted polymer design

Several experimental techniques, which permit the convergent and rationale design of (*E*)-resveratrol imprinted polymers, have been used in these investigations. Molecular modelling techniques based on a method described by Schwarz et al. [31] were employed to estimate the strength of intermolecular interactions between (*E*)-resveratrol and a range of potential functional monomer clusters. This approach identified 4-vinylpyridine as a suitable functional monomer (FM) and predicted that a 3:1 molar ratio of 4VP:(*E*)-resveratrol was optimal for the formation of the most stable pre-polymerisation complex (Fig. 2). These interactions were confirmed by ^{1}H NMR spectroscopy titration analysis, where titration with 4VP resulted in the chemical shift of the phenolic OH groups moving downfield by a total of approximately 0.8 ppm while the other chemical shifts remained constant. This change in spectral properties can be attributed to self-assembly interactions such as those previously observed by Koyama and Wakisaka [32] whereby the interaction of pyridine and phenol leads to the formation of multilayer clusters *via* aromatic intermolecular O–H···N hydrogen bonding interactions. The rationale for the use of CD_3CN for the NMR studies was two-fold. Firstly, in order to assess the molar concentration ranges where most favourable intermolecular template-monomer interactions occurred it was essential to avoid the use of a protic polar solvent, such as ethanol either alone or as a mixture with acetonitrile, since this solvent choice would result in very fast proton exchange rates and as such the monomer–template interactions could not be detected by the ^{1}H NMR measurements. Secondly, a significantly greater amount of template is required for the polymer preparation than is required

Table 2
Binding capacity, imprinting factors and selectivities of (*E*)-resveratrol, **1**, and different structurally related polyphenols, **2**–**8**, (0.5 mM in acetonitrile) towards P1 and N1 under static equilibrium binding conditions without competition. Refer to Fig. 5 for the structural code for the polyphenols **1**–**8**.

Analyte Details given in Fig. 5	MIP P1 binding μmol/g polymer B_{MIP}	NIP N1 binding μmol/g polymer B_{NIP}	Imprinting factor IF (B_{MIP}/B_{NIP})	$B_{MIP} - B_{NIP}$	Selectivity $\alpha = (B_{MIP} - B_{NIP})/B_{NIP}$
1	12.36	5.25	2.35	7.11	1.36
2	19.37	16.59	1.17	2.78	0.17
3	6.11	1.52	4.02	4.6	3.03
4	6.39	2.21	2.89	4.19	1.9
5	2.23	1.42	1.57	0.81	1.94
6	2.66	1.11	2.40	1.56	1.41
7	2.27	0.88	2.60	1.40	1.59
8	0.91	0.47	1.94	0.43	0.92

for the NMR titration studies with the issue of higher solubility of the template in ethanol–acetonitrile mixtures thus not a factor for the titration studies to be satisfactorily conducted in neat CD_3CN. Moreover, as the results shown in Fig. 2 demonstrate, a distinct minimum in the ΔE_i value for the self assembly of the (*E*)-resveratrol into the pre-polymerisation complex is observed at 3 molar equivalents with 4-vinylpyridine. Although the functional monomer acrylamide displayed a slightly more negative ΔE_i value at 6 molar equivalents, our findings are concordant with the preliminary results of Xiang et al. [33], who have reported a lower binding capacity for an AAM-MIP prepared using a randomly selected ratio of 1:6 resveratrol:AAM. Consequently, the more negative ΔE_i value observed from our ^{1}H NMR studies for the AAM-MIP may therefore reflect a higher level of non-specific monomer-to-monomer interactions rather than specific monomer-to-template interactions and this higher level of non-specific binding leads to a less effective MIP.

3.3. Molecularly imprinted polymer preparation

Solid imprinted block copolymers were prepared by incorporating a small percentage of ethanol into the porogen solution (i.e. acetonitrile/ethanol, 5:1, v/v) to increase the solubility of (*E*)-resveratrol without compromising H-bonding capabilities. The presence of this polar protic solvent may enhance the aromatic π–π interactions between aromatic groups already clustered in close proximity, while also stabilising existing interactions within the phenolic–pyridinyl cluster systems in a manner similar to that described by Haupt et al. [34] in their studies with the herbicide, 2,4-dichlorophenoxyacetic acid.

3.4. Molecularly imprinted polymer evaluation

Comparison of binding events observed with the MIP and NIP reference materials revealed the extent to which porogen composition as well as imprinting efficiency affects the adsorption of (*E*)-resveratrol. Fig. 3 shows the binding isotherms derived from static adsorption measurements for polymers P1 and N1 with (*E*)-resveratrol, respectively. The selective capacity ($B_{MIP} - B_{NIP} = 14$ μmol/g) validates an imprinting effect resulting from the successful formation of (*E*)-resveratrol binding cavities or regions within the imprinted polymer. The smaller amounts of (*E*)-resveratrol bound by the non-imprinted control polymer N1 is most likely due to a combination of non-specific surface interactions with the randomly dispersed, but accessible monomer units and the (statistically) fortuitous formation of some cavity-like structures with the correct disposition of the functional binding groups during the generation of the non-imprinted polymer. The binding capacities of MIPs based on self-assembly procedures are known to be variable from preparation to preparation [35]. When these evaluations were conducted using multiple batches of P1 and N1, prepared by similar but not identical conditions, some small variations in the total binding capacity values (up to ±10%) were observed from preparation to preparation, although the selective ($B_{MIP} - B_{NIP}$) capacity values remained essentially constant, suggesting that the imprinting effect is largely unaffected from batch to batch for MIPs prepared with the conditions described above with similar protocols.

Scatchard analysis [36] for the binding data for P1 revealed a nonlinear concave-upward curve with two distinct linear regions. This behaviour is typical of (i) heterogeneity of binding sites, (ii) cooperativity of binding or (iii) multivalent ligand binding, of which (i) is frequently considered to describe the binding of molecules to non-covalently prepared imprinted polymers [37–39]. To confirm that non-specific surface interactions with randomly dispersed 4VP were primarily responsible for the binding response of the non-imprinted polymer N1, the polymers P2 ((*E*)-resveratrol imprinted poly-EGDMA, no FM) and N2 (non-imprinted poly-EGDMA, no FM) were also prepared. The respective binding capacities (related to the affinities) of these polymers for interaction with (*E*)-resveratrol under the same conditions are shown in Fig. 4. As anticipated, polymers P2 and N2 exhibited negligible (*E*)-resveratrol adsorption, indicating that the cross-linker EGDMA does not significantly contribute to the polymer binding responses. A benefit of utilising the polymer N2 is that the role individually played by different types of monomer units with respect to polymer backbone-mediated non-specific binding can be further delineated. Additionally, the failure of P2 to recognise (*E*)-resveratrol suggests that the presence of cavities of similar size and shape as (*E*)-resveratrol alone is insufficient to ensure that strong binding will occur allowing the molecule to be actively captured from solution. Rather, these findings highlight the importance for the complementary functional groups to be positioned vectorially in the appropriate orientation within the cavity site in addition to the size of the cavity *per se*.

Table 3
Competitive cross-reactivity towards an (*E*)-resveratrol MIP using a solution containing (*E*)-resveratrol, **1**, and several closely related polyphenol analogues, **2**–**8**. Refer to Fig. 5 for the structural code for the polyphenols **1**–**8**.

Analyte	MIP binding μmol/g polymer B_{MIP}	NIP binding μmol/g polymer B_{NIP}	Imprinting factor IF (B_{MIP}/B_{NIP})	$B_{MIP} - B_{NIP}$	Selectivity $\alpha = (B_{MIP} - B_{NIP})/B_{NIP}$
1	7.78	3.45	2.26	4.33	1.26
2	19.84	14.08	1.41	5.77	0.41
3	3.70	2.01	1.84	1.69	0.84
4	3.5	1.9	1.84	1.6	0.84
6	1.17	0.8	1.46	0.38	0.47
8	1.00	1.31	0.76	−0.3	−0.23

Single analyte (non-competitive) cross reactivity studies were employed to examine the influence of positions and numbers of hydrogen bonding OH groups present on the target molecule upon molecular recognition. The static binding affinities of (*E*)-resveratrol and a range of structural analogues towards the (*E*)-resveratrol imprinted polymer P1 were determined using equilibrium binding methods. The concentration of the bound analyte was determined by the difference between the initial analyte concentration and the concentration of remaining analyte in solution (Fig. 5 and Table 2). This analysis showed that the number of phenolic OH groups within the target molecule clearly influenced the amount of specific binding to P1 and non-specific binding to N1. For example, the tetra-ol **2** displaying high levels of affinity to both P1 and N1. Analytes with fewer than three phenolic OH groups displayed minimal affinity to N1 ($\leq$2.21 μmol/g). This observation is similar to that reported for an amino acid imprinted system [40], whereby non-template analytes possessing a greater number of functional groups displayed higher non-specific binding with randomly dispersed functional groups within the polymer matrix. The best binding was observed for P1 with the template (*E*)-resveratrol with binding capacity of 12.36 μmol/g and an imprinting factor (IF) (where IF = B_{MIP}/B_{NIP}) of 2.35.

Analogues of (*E*)-resveratrol having one less phenolic OH group (e.g. analytes **3** and **4**) demonstrated a reduction in the extent of analyte binding by approximately 50% of that observed for (*E*)-resveratrol, yet resulted in relatively higher recognition (IF = 4.02 and 2.89, respectively), as non-specific binding of these molecules was significantly reduced. (*E*)-resveratrol analogues having two less phenolic OH groups (e.g. analytes **6** and **7**) demonstrated further reduced specific binding to P1, with essentially no difference conferred by the relative position of the OH group. Binding of the (*E*)-stilbene **8** to P1 was effectively abolished due to the absence of phenolic OH groups. Interestingly, the binding of the naturally occurring mono glycosylated derivative, (*E*)-resveratrol-3-β-D-glucopyranoside **5**, to P1 paralleled that observed for the monophenolic (*E*)-resveratrol analogues **6** and **7**. The presence of the bulky glucose group presumably prevented the interaction of the *meta* positioned OH group within the binding cavity, thereby leaving the *para* positioned OH group as the only functionality capable of hydrogen bonding.

The binding of polyphenol analogues to polymer P1 was also investigated under competitive conditions. Results from these competitive static cross-reactivity binding experiments employing an equimolar mixture of (*E*)-resveratrol **1** and analogues **2**, **3**, **4**, **6** and **8** at 0.5 mM each are shown in Table 3. To reduce the complexity of the mixture, analogues **5** and **7** were not included in this mixture since these analogues had been previously shown (as discussed above) to have negligible affinity for P1. Polymer P1 retained good recognition for (*E*)-resveratrol with imprinting factor (IF 2.26) and selectivity (α 1.26) (where $\alpha = (B_{MIP} - B_{NIP})/B_{NIP}$) parameters that were virtually unchanged from the single analyte experiment (IF 2.35, α 1.36). This result clearly demonstrates that P1 preferentially binds (*E*)-resveratrol over its structurally similar analogues. The binding capacity of P1 for (*E*)-resveratrol from the mixture was reduced (7.78 μmol/g), which may be a consequence of competition for available binding sites by the tetra-ol analogue, **2**. In contrast, the tetra-ol analogue **2** displayed unchanged binding capacity to P1 (19.84 μmol/g) with improved recognition (IF 1.41) and selectivity (α 0.41) compared to the non-competitive studies (19.37 μmol/g, IF 1.17, α 0.17). The increased IF may be a consequence of reduced non-specific binding of analogue **2** to randomly distributed 4VP throughout the polymer arising from non-specific binding of other analytes present in the mixture to these sites. The (*E*)-resveratrol analogues **3** and **4**, which displayed good recognition in single analyte assays (IF 4.02 and 2.89, respectively) were unable to compete with (*E*)-resveratrol **1** and compound **2** for available binding sites on P1, as manifested by the reduced IF and α values for both analogues. Consistent with the earlier static binding results described above for single analytes, compounds **6** and **8** demonstrated essentially negligible binding. Compound **8** continued to show the lowest value consistent with the least amount of recognition. These results, in accordance with those obtained for single analyte assays, emphasise the importance of the –OH groups with respect to their number and position in the core structure of the target molecule. Analogues of (*E*)-resveratrol having at least two –OH groups in the *meta* and/or *para* positions on the aromatic rings (compounds **1**, **2**, **3**, **4**) clearly demonstrated moderate to good affinity, with good correlation between binding affinities and the number of aromatic-linked OH groups present.

4. Conclusion

A set of (*E*)-resveratrol-imprinted polymers have been prepared *via* non-covalent self-assembly procedures and shown with both single and mixed analyte samples to have a highly specific molecular recognition for the template over similar polyphenolic analogues. The extent of molecular recognition of the compounds was influenced by the presence of aromatic OH groups, with at least two such groups in the *meta* and or *para* positions required. Compounds with more than three aromatic OH groups exhibited strong affinity for the (*E*)-resveratrol imprinted polymer, but their molecular recognition was inhibited by a high level of non-specific binding. Superior recognition was observed for (*E*)-resveratrol which was able to interact with the binding cavity through three *meta* and *para* positioned aromatic OH groups having complementarity with the 3-dimensional binding cavity

Acknowledgement

The authors gratefully acknowledge the financial support from the CSIRO National Research Food Futures Flagship.

References

[1] K.A. Steinmetz, J.D. Potter, J. Am. Diet. Assoc. 96 (1996) 1027.
[2] R. Miyazaki, T. Ichiki, T. Hashimoto, K. Inanaga, I. Imayama, J. Sadoshima, K. Sunagawa, Arterioscler. Thromb. Vasc. Biol. 28 (2008) 1263.
[3] D.R. Valenzano, A. Cellerino, Cell Cycle 5 (2006) 1027.
[4] D.R. Valenzano, E. Terzibasi, T. Genade, A. Cattaneo, L. Domenici, A. Cellerino, Curr. Biol. 16 (2006) 296.
[5] K.T. Howitz, K.J. Bitterman, H.Y. Cohen, D.W. Lamming, S. Lavu, J.G. Wood, R.E. Zipkin, P. Chung, A. Kisielewski, L.L. Zhang, B. Scherer, D.A. Sinclair, Nature 425 (2003) 191.
[6] M.S. Jang, E.N. Cai, G.O. Udeani, K.V. Slowing, C.F. Thomas, C.W.W. Beecher, H.H.S. Fong, N.R. Farnsworth, A.D. Kinghorn, R.G. Mehta, R.C. Moon, J.M. Pezzuto, Science 275 (1997) 218.
[7] Y.J. Surh, Mutat. Res. Fundam. Mol. Mech. Mutagen. 428 (1998) 305.
[8] Y.J. Surh, Y.J. Hurh, J.Y. Kang, E. Lee, G. Kong, S.J. Lee, Cancer Lett. 140 (1999) 1.
[9] C.S. Huang, W.Y. Ma, A. Goranson, Z.G. Dong, Carcinogenesis 20 (1999) 237.
[10] N. Richard, D. Porath, A. Radspieler, J. Schwager, Mol. Nutr. Food Res. 49 (2005) 431.
[11] A.R. Martin, I. Villegas, C. La Casa, C.A. de la Lastra, Biochem. Pharmacol. 67 (2004) 1399.
[12] I. Lekli, G. Szabo, B. Juhasz, S. Das, M. Das, E. Varga, L. Szendrei, R. Gesztelyi, J. Varadi, I. Bak, D.K. Das, A. Tosaki, Am. J. Physiol. Heart Circul. Physiol. 294 (2008) H859.
[13] S. Das, G.A. Cordis, N. Maulik, D.K. Das, Am. J. Physiol. Heart Circul. Physiol. 288 (2005) H328.
[14] R. Hattori, H. Otani, N. Maulik, D.K. Das, Am. J. Physiol. Heart Circul. Physiol. 282 (2002) H1988.
[15] K. Inanaga, T. Ichiki, H. Matsuura, R. Miyazaki, T. Hashimoto, K. Takeda, K. Sunagawa, Hypertens. Res. 32 (2009) 466.
[16] P. Jeandet, M. Sbaghi, P. Meunier, Vitis 34 (1995) 91.
[17] R.E. King, J.A. Bomser, D.B. Min, Comp. Rev. Food Sci. Food Saf. 5 (2006) 65.
[18] P. Langcake, R.J. Pryce, Physiol. Plant Pathol. 9 (1976) 77.
[19] V.S. Sobolev, R.J. Cole, J. Agric. Food Chem. 47 (1999) 1435.
[20] T.H. Sanders, R.W. McMichael, K.W. Hendrix, J. Agric. Food Chem. 48 (2000) 1243.
[21] R.M. Lamuela-Raventos, A.I. Romero-Perez, A.L. Waterhouse, M.C. de la Torre-Boronat, J. Agric. Food Chem. 43 (1995) 281.

[22] F. Mattivi, Zeitschrift für Lebensmitteluntersuchung und -Forschung A (1898–1999) 196 (1993) 522.
[23] A.I. Romero-Perez, R.M. Lamuela-Raventos, C. Andres-Lacueva, M.C. de la Torre-Boronat, J. Agric. Food Chem. 49 (2001) 210.
[24] A. Chafer, M. Pascual-Marti, A. Salvador, A. Berna, J. Sep. Sci. 28 (2005) 2050.
[25] C. Alexander, H.S. Andersson, L.I. Andersson, R.J. Ansell, N. Kirsch, I.A. Nicholls, J. O'Mahony, M.J. Whitcombe, J. Mol. Recognit. 19 (2006) 106.
[26] J.Z. Hilt, M.E. Byrne, Adv. Drug Deliv. Rev. 56 (2004) 1599.
[27] F.L. Dickert, P.A. Lieberzeit, O. Hayden, S. Gazda-Miarecka, K. Halikias, K.J. Mann, C. Palfinger, Sensors 3 (2003) 381.
[28] C. Baggiani, L. Anfossi, C. Giovannoli, Anal. Chim. Acta 591 (2007) 29.
[29] M.T.W. Hearn, S. Langford, K.L. Tuck, S. Harris, R.I. Boysen, V.T. Perchyonok, B. Danylec, L. Schwarz, J. Chowdhury, PCT Int. Appl. 269 (2010), WO2010085851.
[30] M.B. Andrus, J. Liu, E.L. Meredith, E. Nartey, Tetrahedron Lett. 44 (2003) 4819.
[31] L. Schwarz, C.I. Holdsworth, A. McCluskey, M.C. Bowyer, Aust. J. Chem. 57 (2004) 759.
[32] T. Koyama, A. Wakisaka, J. Chem. Soc. Faraday Trans. 93 (1997) 3813.
[33] H.-Y. Xiang, C.-S. Zhou, S.-A. Zhong, Q.-F. Lei, Yingyong Huaxue 22 (2005) 739.
[34] K. Haupt, A. Dzgoer, K. Mosbach, Anal. Chem. 70 (1998) 628.
[35] K. Booker, M.C. Bowyer, C.J. Lennard, C.I. Holdsworth, A. McCluskey, Aust. J. Chem. 60 (2007) 51.
[36] G. Scatchard, Ann. N. Y. Acad. Sci. 51 (1949) 660.
[37] J. Matsui, Y. Miyoshi, O. Doblhoff-Dier, T. Takeuchi, Anal. Chem. 67 (1995) 4404.
[38] X. Li, M. Husson Scott, Biosens. Bioelectron. 22 (2006) 336.
[39] I.R.J. Umpleby, S.C. Baxter, M. Bode, J.K. Berch, R.N. Shah, K.D. Shimizy, Anal. Chim. Acta 435 (2001) 35.
[40] H. Kim, G. Guiochon, Anal. Chem. 77 (2005) 6415.